Available online at www.sciencedirect.com
ScienceDirect
Biochimica et Biophysica Acta 1774 (2007) 772–780
Biochimica et Biophysica Acta
BBA
www.elsevier.com/locate/bbapap

Thermal unfolding of human BRCA1 BRCT-domain variants

George Nikolopoulos [a,b], Serapion Pyrpassopoulos [a], Angelos Thanassoulas [a], Persefoni Klimentzou [a], Christos Zikos [a], Metaxia Vlassi [a], Constantinos E. Vorgias [c], Drakoulis Yannoukakos [a], George Nounesis [a,*]

[a] *National Centre for Scientific Research "Demokritos", 153 10 Aghia Paraskevi, Greece*
[b] *Biogenomica, Centre for Genetic Research and Analysis, 152 32 Halandri, Greece*
[c] *Department of Biology, National and Kapodistrian University of Athens, 157 84 Zografou, Greece*

Received 12 February 2007; received in revised form 21 March 2007; accepted 26 March 2007
Available online 6 April 2007

Abstract

Missense mutations at the BRCT domain of human BRCA1 protein have been associated with an elevated risk for hereditary breast/ovarian cancer. They have been shown to affect the binding site and they have also been proposed to affect domain stability, severely hampering the protein's tumor suppressor function. In order to assess the impact of various such mutations upon the stability and the function of the BRCT domain, heat-induced denaturation has been employed to study the thermal unfolding of variants M1775R and R1699W, which have been linked with the disease, as well as of V1833M, which has been reported for patients with a family history. Calorimetric and circular dichroism results reveal that in pH 9.0, 5 mM borate buffer, 200 mM NaCl, analogously to wild type BRCT, all three variants undergo partial thermal unfolding to a denatured state, which retains most of the native's structural characteristics. With respect to wild-type BRCT, the mutation M1775R induces the most severe effects especially upon the thermostability, while R1699W also has a strong impact. On the other hand, the thermal unfolding of variant V1833M is only moderately affected relative to wild-type BRCT. Moreover, isothermal titration calorimetric measurements reveal that contrary to M1775R and R1699W variants, V1833M binds to BACH1 and CtIP phosphopeptides.
© 2007 Elsevier B.V. All rights reserved.

Keywords: BRCA1-BRCT domain; Thermal unfolding; DSC; CD; ITC; V1833M; M1775R; R1699W

1. Introduction

A large number of germ-line mutations in the human *BRCA1* gene have been linked with inherited breast and ovarian cancer [1,2]. Most are frame shift or nonsense mutations, which can straightforwardly be assigned as deleterious since they lead to truncated proteins. On the other hand, over one hundred missense mutations located in the BRCT domain, detected from genetic screening worldwide, have been deposited at the Breast Cancer Information Core (BIC) as unclassified variants. *In vitro* functional studies have shown that quite a few can cause loss of the protein's function [3–6], while co segregation analysis has revealed the association of a handful of these missense mutations to hereditary breast/ovarian cancer.

The crystal structures of the tandem BRCT repeats (each containing ~90 aminoacids) comprising the C-terminal functional BRCT domain of BRCA1 [7] as well as of 53BP1 [8], reveal a common structural motif, which is highly conserved among BRCT repeats. It consists of a parallel four-stranded β-sheet located at the central part of the fold surrounded by three α-helices. The two BRCT repeats pack together in a specific head-to-tail manner, giving rise to the formation of a conserved, almost all-hydrophobic inter-repeat interface. A flexible, BRCT-repeat-interconnecting, 23-residue linker is also involved in the interface formation since the α-helix at its center packs right against the inter-BRCT interface. The structural integrity of the tandem repeats is essential for the molecule's interaction with phosphorylated protein targets [9] including the DNA helicase BACH1 and the CtBP-interacting protein CtIP [10]. The binding of the BRCA1 BRCT domain to BACH1 and the transcriptional corepressor CtIP plays an important role in the control of the

* Corresponding author. Tel.: +30 210 6503857; fax: +30 210 6543526.
E-mail address: nounesis@rrp.demokritos.gr (G. Nounesis).

1570-9639/$ - see front matter © 2007 Elsevier B.V. All rights reserved.
doi:10.1016/j.bbapap.2007.03.018

G2/M phase checkpoint [11], [12]. The crystal structure of the BRCT complex with the phosphopeptides containing the sequence pSer-X-X-Phe, (phosphorylation of Ser990 and Ser327 for the BACH1 and CtIP phosphopetides respectively, X stands for any residue [13–16]) revealed that phosphoserine binds at a conserved pocket at the N-terminal BRCT repeat while the hydrophobic groove at the inter-BRCT interface region recognizes phenylalanine. A higher affinity of the BRCT domain has been shown for BACH1 than CtIP due to the interactions of the neighboring aminoacids [16]. Missense mutations at the BRCT domain have been proposed to induce the molecule's loss of function by directly altering the binding sites and/or by destabilization. Characteristically, NMR structural results of the BRCT-domain suggest that for biologically active conformations the proper alignment of the N and C-terminal BRCT repeats is essential [17].

The cancer-linked BRCT missense mutation M1775R cripples the DNA repair and transcription function of BRCA1 [18,19] and inhibits BRCT interactions with the DNA helicase BACH1 [20] as well as with the transcriptional co-repressor CtIP [21,22]. Met1775 is located at the inter-BRCT-repeat interface. It is well conserved among the available BRCA1 BRCT domain orthologs. The crystal structure of the M1775R mutant revealed that the methionine–arginine substitution leads to a disruption of the hydrogen-bond network at the inter-BRCT-repeat interface [23]. Direct comparisons with the crystallographic studies of the BRCT-phosphopeptide complex [15] demonstrated that Arg1775, blocks access of the peptide-Phe(+3) (Phe993 for BACH1 and Phe330 for CtIP) to the hydrophobic inter-BRCT-repeat groove.

Residue Arg1699 is highly conserved and it too is located at the inter-BRCT-repeat interface region. It participates in the formation of a salt bridge between the N and C-terminal BRCT repeats. The arginine to tryptophan substitution leads to the loss of salt-bridging interactions while inducing steric strain associated with the accommodation of the tryptophan residue [23]. Moreover, Arg1699 is part of the sides of the pocket recognizing the Phe(+3) peptide residue, playing an important role in the alignment of the main chain of Phe(+3) [15].

The variant V1833M has only been reported in BIC three times, one of which concerns a Greek family with two ovarian cancer incidents [24]. Val1833 is highly conserved and although the substitution to methionine is predicted to be a mild one [3], a possible destabilization of the overall fold has been suggested [25] since Val1833 is located in the hydrophobic core of the C-terminal BRCT repeat. Interestingly, chemical denaturation experiments have shown that the valine to methionine substitution reduces the thermodynamic stability of the BRCT domain with respect to an intermediate fold, exhibiting an almost complete loss of structural features, by approximately 5.5 kcal/mol [26]. Destabilization of the overall fold has also been proposed for A1708E located right in the hydrophobic inter-repeat interface and G1738R at the inter-repeat linker.

Thermal denaturation experiments of the BRCT domain of human BRCA1 have shown that the unfolding of the protein occurs via an aggregation-prone partly unfolded denatured state that is structurally very similar to the native [27]. Here we present thermal unfolding results for variants M1775R, R1699W, and V1833M obtained via high-sensitivity differential scanning calorimetry (DSC) and circular dichroism (CD). For all three variants we show that heat-induced denaturation always involves a partly unfolded, denatured state, which retains most of the native's secondary structural characteristics. The three mutations have varying effects upon the molecule's thermostability with respect to wild type, depending on their location relative to the hydrophobic inter-BRCT-repeat interface. Moreover, isothermal titration calorimetric studies demonstrate that contrary to M1775R and R1699W variants, V1833M binds to both the BACH1 and the CtIP phosphopeptides.

2. Materials and methods

2.1. Gene subcloning and mutagenesis

The encoding region for human wild type and mutant A1708E, BRCA1 BRCT-tan domain (a.a. 1646–1859) were amplified by PCR from plasmids kindly provided by Prof. A.N. Monteiro (Cornell University), using the following primers: (i) BRCT (*Nde*I), ACATATGGTCAACAAAAGAATGTGCATGGTG and (ii) BRCT (*Bam*HI), AGGATCCTCAGGGGATCTGGGGTATCAGG with *Nde*I and *Bam*HI restriction sites at their 5′ and 3′ ends, respectively. The resulting 750 bp PCR products were ligated into pCR2.1 cloning vector and transformed into *Escherichia coli* INVaF′ according to the manufacturer's instructions (Invitrogen). Construction of G1738R, M1775R, R1699W and V1833M mutants was obtained using the pCR2.1-cloning vector containing the residues 1646–1859 of human BRCA1 coding sequence as described previously [27]. The mutations were generated using the QuickChange site-directed mutagenesis kit (Stratagene) and the primers listed in Table 1.

The PCR products were digested with *Dpn*I and transformed into Novablue competent cells (Novagen). Automated DNA sequencing was employed to

Table 1
Forward (f) and reverse (r) primers used for the generation of specific mutations at the BRCT domain

Mutation	Primer
R1699Wf	GAGTTTGTGTGTGAA**T**GGACACTGAAGTATTTTCTAGGAATTG
R1699Wr	CAATTCCTAGAAAATACTTCAGTGTCC**A**TTCACACACAAACTC
G1738Rf	GATTTTGAAGTCAGA**C**GAGATGTGGTCAATGGAAG
G1738Rr	CTTCCATTGACCACATCTC**G**TCTGACTTCAAAATC
M1775Rf	TATGGGCCCTTCACCAACA**GA**CCCACAGATCAACTGG
M1775Rr	CCAGTTGATCTGTGGG**TC**TGTTGGTGAAGGGCCCATA
V1833Mf	ATGTGTGAGGCACCT**A**TGGTGACTCGAGAGTGGGTGTTG
V1833Mr	CAACACCCACTCTCGAGTCACCA**T**AGGTGCCTCACACAT

Framed bases indicate the substitutions leading to the respective variants.

identify the successful clones using the ABI310 sequencer (Applied Biosystems). Plasmids isolated from a positive clone were submitted to digestion with *Nde*I and *Bam*HI and the inserts were cloned into pET-3a expression vector (Novagen) and transformed into Novablue competent cells. Plasmids DNA isolated from the positive clones were then transformed into *E. coli* BLR(DE3)pLysS expression strain (Novagen).

2.2. Protein expression and purification

The BRCT variants R1699W, A1708E, G1738R, M1775R and V1833M were overproduced in *E. coli* BLR(DE3)pLysS strain, which was grown at 37 °C in LB medium containing 50 mM ampicillin and 50 mM chloramphenicol to an $OD_{600\ nm}$ ~0.7. Protein expression was performed at 24 °C (BRCT-M1775R, BRCT-A1708E, BRCT-G1738R), 28 °C (BRCT-V1833M) and at 18 °C (BRCT-R1699W) upon induction with 0.5 mM isopropyl β-D-thiogalactoside (IPTG) for 5 h. Cells were harvested by centrifugation and lysed in 20 mM Na-Phosphate (pH 6), 75 mM NaCl, 1 mM EDTA (pH 8.5), 1 mM phenylmethylsulfonyl fluoride (PMSF), 0.5% Triton X-100 and 1 mM β-mercaptoethanol. Cells were lysed at 4 °C using an UP 200 S HIELSCHER homogenizer. After centrifugation at 15,000×*g* and 4 °C for 25 min, the soluble fraction of the proteins was isolated and purified using a combination of SP-Sepharose Fast Flow and a Q-Sepharose High Performance column (Pharmacia). Protein concentration was measured spectrophotometrically at 280 nm. SDS-PAGE analysis was carried out according to Laemmli [28].

2.3. Gel filtration chromatography

Gel filtration chromatography experiments were carried out on a Superose™ 12 prepacked HR 10/30 column (Amersham Biosciences). The column was run with an FPLC® system at a flow rate of 0.4 ml/min. The sample volume loaded each time was 0.2 ml. The absorption (A) of the eluent was monitored at 280 nm.

2.4. Circular dichroism spectroscopy (CD)

CD measurements were conducted using a JASCO-715 spectropolarimeter with a Peltier type cell holder, which allows for temperature control. Wavelength scans in the far (190 to 260 nm) and the near (260 to 340 nm) UV regions were performed in Quartz SUPRASIL (HELLMA) precision cells of 0.1 cm and 1 cm path length respectively. Each spectrum was obtained by averaging five to eight successive accumulations with a wavelength step of 0.2 nm at a rate of 20 nm min^{-1}, response time 1 s and band width 1 nm. Buffer spectra were accumulated and subtracted from the sample scans. The absorption spectra were recorded selecting the UV (single) mode of the instrument. Spectra for the denatured states of the molecules involved in present study have been obtained at ~55 °C, which is approximately 5 degrees higher than the denaturation temperature of wild-type BRCT. For all the samples studied, no changes in the CD spectra have been recorded at various temperatures higher than the denaturation temperature, which is significant of the fact that no CD-detectable aggregation takes place. Prior to high-temperature data acquisition the samples where allowed to equilibrate at 55 °C for 15–20 min.

2.5. Differential scanning calorimetry (DSC)

For the high-sensitivity calorimetric measurements the VP DSC calorimeter was employed (Microcal, Northampton, USA) [29]. Protein solutions in pH 9.0, 5 mM borate buffer, 200 mM NaCl were used in the DSC studies. Concentrations varied between 0.2 and 0.3 mg/ml for wt-BRCT, 0.2 and 0.4 mg/ml for the BRCT-M1775R variant, 0.2 mg/ml and 0.3 mg/ml for BRCT-V1833M and between 0.3 mg/ml and 0.4 mg/ml for BRCT-R1699W. Protein samples and buffer reference solutions were properly degassed and carefully loaded into the cells to avoid bubble formation. Four to five reference scans with buffer filled cells (sample and reference cell volume is 0.523 ml) preceded each sample run in order to achieve near perfect baseline repeatability. A typical DSC experiment consisted of a heating scan at a programmed heating rate followed by a second heating scan, which probed the irreversibility of the transitions under study. The difference in the heat capacity between the initial and final states was modelled by a sigmoidal chemical baseline [30].

2.6. Isothermal titration calorimetry (ITC)

The interaction of wt-BRCT and the three variants with the BACH1 phosphopeptide ISRSTpSPTFNKQ and the CtIP phosphopeptide PTRVSpSPVFGAT have been studied at 20 °C in pH 9.0, 5 mM borate buffer, 200 mM NaCl solutions, using a MCS-ITC calorimeter (Microcal, Northampton, USA). The protein concentration used for the experiments was 0.019 ± 0.003 mM and the ligand concentration was 0.21 ± 0.02 mM. For wt-BRCT and the variant V1833M experiments have also been carried out at pH 7.0 10 mM Na-phosphate buffer. All the ITC experiments were designed in series of twenty-four 10-μL injections allowing 300 s between consecutive injections at constant 400 rpm stirring. All the ITC experiments have been reproduced at least three times. From the raw exothermic heat pulse data for each injection, the instrumental baseline was subtracted before obtaining normalized integrated heat vs. molar ratio data from which the corresponding dilution heat, measured separately for each phosphopeptide, has also been subtracted. All the ITC control experimental runs have been repeated twice. The isothermal titration curves, thus obtained were fitted using ORIGIN® built-in functions for a single-site binding model providing values for the stoichiometry N, the binding constant k_a and the enthalpy change ΔH.

3. Results

The BRCT domain variants R1699W, M1775R and V1833M were expressed in *E. coli*. They were obtained in highly soluble form, more than 99% pure and stable for several days at 4 °C. SDS-PAGE showed the presence of a single band at the expected MW ~25 kDa. The three mutated residues are shown in the BRCT structure presented in Fig. 1 [7]. While Met1775 and Arg1699 are both located at the hydrophobic interface between the two BRCT repeats formed by the packing of three helices: α2 (of the N-terminal BRCT repeat) and α1′ α3′ (of the C-terminal BRCT repeat), Val1833 is located at the β4′ strand which is part of the central hydrophobic core of the C-terminal BRCT repeat. It is noteworthy, that we have also expressed the variants A1708E and G1738R. Both these variants were insoluble and thus impossible to study via DSC or CD.

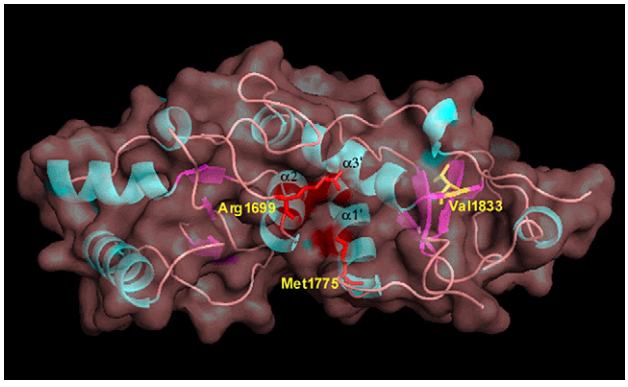

Fig. 1. Ribbon representation with transparent space-filling overlay of the structure of the BRCT domain of human BRCA1 adapted from Williams et al. [7], (RCSB entry: 1JNX). The three helices participating in the hydrophobic inter-BRCT-interface region are labeled, (the two C-terminal BRCT-repeat helices are labeled with 'prime'). Residues, mutations of which are being studied are depicted either in red (M1775, R1699) to indicate existing evidence linking them to hereditary breast/ovarian cancer, or yellow (V1833). (For interpretation of the references to colour in this figure legend, the reader is referred to the web version of this article.)

3.1. DSC

Heat-induced denaturation studies of wt-BRCT published previously, have shown that two important factors limit our ability for a full thermodynamic investigation [27]. First, pH-dependent aggregation in the thermally denatured state can severely distort the shape of the DSC thermal unfolding irreversible peaks and second, there exists a buffer-sensitive oligomerization of wt-BRCT in the native state which may well complicate the analysis of the calorimetric results [27]. In order to optimize the quality of the experimental data and carry out the measurements of the BRCT variants presented here, we have found as suitable experimental conditions for the thermal unfolding BRCA1-BRCT solutions in pH 9.0, 5 mM sodium borate buffer, 200 mM NaCl. As illustrated in Fig. 2, gel filtration chromatography reveals that in this buffer, wt-BRCT as well as the three variants are all in a monomeric native state. Moreover, since the pH of this buffer is relatively temperature-independent, it allows for direct comparison of the calorimetric results without incorporating unpredictable effects induced by pH variations. Finally, as shown in Fig. 3, the DSC thermograms exhibit no obvious signs of aggregation-induced artifacts.

The high-accuracy DSC results for wild-type BRCT (wt-BRCT) at pH 9.0, 5 mM sodium borate buffer, 200 mM NaCl are presented in Table 2. The heat capacity ($<\Delta C_p>$) vs. temperature (T) profiles for the thermal denaturation of wt-BRCT are described by a single endothermic, irreversible peak (Fig. 3) at T_m, (the temperature corresponding to maximum $<\Delta C_p>$)=48.3±0.5 °C measured at heating scan rate u=1.5 K/min. As in the case of wt-BRCT at pH 9.0, 10 mM Tris–HCl, 20 mM NaCl, while the $<\Delta C_p>$ vs. T profiles are irreversible, rate-dependent measurements reveal that the denaturation process is characterized by a slow irreversible step and thus the data obtained at highest possible DSC scan rates are likely to exhibit limited kinetic distortions [27]. The value for the enthalpy change is $(\Delta H)_{cal}$ ~87.1±6.4 kcal/mol, for a sample with C_t=0.2 mg/ml, independent of u and for ΔC_p, the heat capacity difference between the denatured and the native state is ΔC_p=0.68±0.15 kcal/K mol. In agreement with the gel filtration chromatography results, there is no dependence between T_m and the concentration C_t, confirming that native wt-BRCT is in a monomeric state. Notably, the results for wt-BRCT in borate buffer compare well with the previously published data obtained in Tris–HCl where wt-BRCT is in a dimeric native state [27].

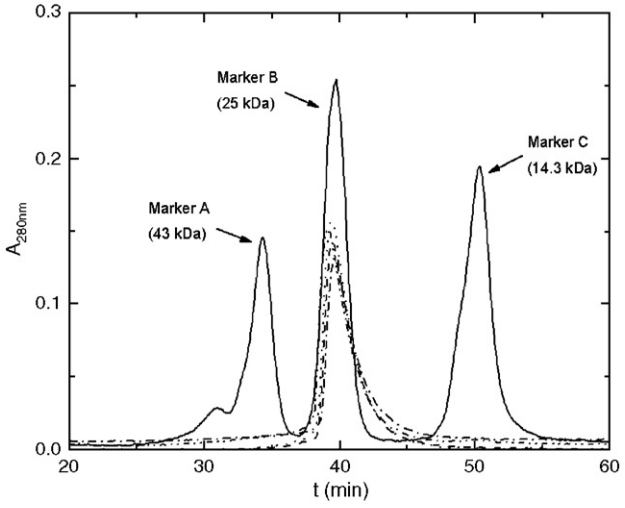

Fig. 2. Gel Filtration experiments on Superose™ 12: In 5 mM sodium borate buffer pH 9.0, 200 mM NaCl, the wild-type as well as the three BRCT variants elute as sharp peaks at a molecular weight corresponding to the monomer (25 kDa). The solid line monitors the elution profile of three markers. The peak marked as A corresponds to Ovalbumin (43 kDa), the peak marked as B corresponds to Chymotrypsinogen A (25 kDa) and the peak marked as C corresponds to Lysozyme (14.3 kDa). The markers were obtained from Sigma Aldrich. Dashed line corresponds to wt-BRCT, dotted line to M1775R, dash-dotted line to R1699W and dash-dot-dotted line to V1833M.

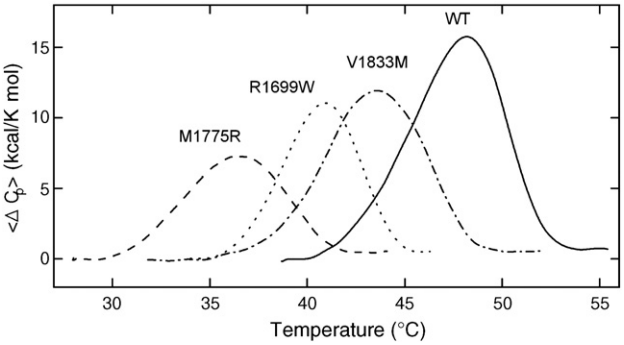

Fig. 3. DSC profiles ($<\Delta C_p>$ vs. T) for the thermally induced denaturation of wt-BRCT and of the three missense variants M1775R, R1699W and V1833M. All the profiles have been obtained at identical solution conditions (pH 9.0, 5 mM sodium borate buffer, 200 mM NaCl) and DSC heating rate u=1.5 K/min. The concentration for all the DSC thermograms presented here was C_t=0.3 mg/ml.

3.1.1. M1775R

The obtained DSC thermograms for the heat denaturation of M1775R variant, for u=1.5 K/min are also presented in Fig. 3. Analogously to the findings for the thermal unfolding of wt-BRCT, the $<\Delta C_p>$ vs. T profiles in pH 9.0, 5 mM sodium borate

Table 2
DSC results

Sample	C_t (mg/ml)	T_m (°C)	$(\Delta H)_{cal}$ (kcal/mol)	ΔC_p (kcal/K mol)
wt-BRTC	0.2	48.3±0.5	87.1±6.4	0.68±0.15
wt-BRTC[a]	0.3	48.3±0.5	81.0±6.5	–
M1775R	0.2	36.7±0.4	43.4±4.2	0.45±0.10
M1775R	0.3	36.3±0.4	44.0±4.2	0.47±0.10
M1775R[a]	0.4	36.6±0.4	40.9±4.1	–
R1699W	0.2	40.9±0.5	51.9±4.5	0.49±0.12
R1699W	0.3	40.7±0.5	47.8±4.4	0.49±0.12
V1833M	0.3	43.5±0.5	74.0±5.3	0.55±0.18
V1833M[a]	0.4	43.7±0.5	73.5±5.1	–

Experimental results for T_m, $(\Delta H)_{cal}$ and ΔC_p for the thermal unfolding of wt-BRCT and the three variants M1775R, R1699W, and V1833M at pH 9.0, 5 mM borate buffer, 200 mM NaCl, for DSC heating scan rate u=1.5 K/min and various protein concentrations C_t.

[a] ΔC_p could not be experimentally determined from the DSC traces.

buffer, 200 mM NaCl were adequately free from aggregation-induced distortions. For all the samples studied, the thermal denaturation of the M1775R variant was irreversible. Calorimetric results obtained for different C_t values are included in Table 2. For all the concentrations (C_t=0.2, 0.3 and 0.4 mg/ml) studied $(\Delta H)_{cal}$ ~42.5 kcal/mol and T_m ~36.5 °C were found to be independent of C_t as well as of u. The value of ΔC_p ~0.46 kcal/K mol was also found to be constant for C_t=0.2 and 0.3 mg/ml. In the case of C_t=0.4 mg/ml though, the value of ΔC_p could not be accurately determined due to aggregation effects affecting the DSC trace in the denatured state. As T_m is found to be independent of C_t, a monomeric native state is evidenced and the denaturation may be modeled by the sequence $N(M1775R) \underset{k_{-1}}{\overset{k_1}{\rightleftarrows}} D \xrightarrow{k_2} I$. Rate-dependent data provide evidence that the irreversible step is slow and that at u=1.5 K/min the thermal unfolding is not far from equilibrium-like conditions. Comparing the calorimetric results for M1775R variant to those for wt-BRCT, it can readily be deduced that while the ΔC_p measurements are comparable, $(\Delta H)_{cal}$ and T_m are considerably affected. $(\Delta H)_{cal}$ is approximately half of the corresponding enthalpic content for the denaturation of wt-BRCT and T_m exhibits a very significant downwards shift by almost 10 degrees.

3.1.2. R1699W

The calorimetric profiles for variant R1699W at pH 9.0, 5 mM sodium borate buffer, 200 mM NaCl are also presented in Fig. 3. These results exhibit characteristic similarities with the corresponding $<\Delta C_p>$ calorimetric traces for M1775R including the irreversibility of the endothermic peaks, the downward T_m-shifts with respect to wt-BRCT and the lack of any C_t-dependence of the experimental T_m values. All the calorimetric parameters obtained for R1699W are listed in Table 2. T_m is shifted downwards by approximately 7.5 °C with respect to wt-BRCT, while ΔC_p=0.49 kcal/K mol and $(\Delta H)_{cal}$ ~50 kcal/mol are comparable to the findings for the M1775R BRCT domain variant. The lack of a C_t -dependence of the experimental T_m values is indicative of a monomeric native state of R1699W in agreement with the gel filtration results. Thermal unfolding is thus likely to follow $N(R1699W) \underset{k_{-1}}{\overset{k_1}{\rightleftarrows}} D \xrightarrow{k_2} I$.

3.1.3. V1833M

Fig. 3 displays the characteristic DSC thermograms for the denaturation of V1833M mutant at pH 9.0, 5 mM sodium borate buffer, 200 mM NaCl, at u=1.5 K/min. Once again the thermal unfolding is irreversible characterized by a single $<\Delta C_p>$ vs. T endothermic peak. The calorimetric results for $(\Delta H)_{cal}$, ΔC_p and T_m are listed in Table 2. Analogously to wt-BRCT as well as to M1775R and R1699W variants, the experimental values obtained for V1833M for $(\Delta H)_{cal}$=74.0±5.3 kcal/mol and ΔC_p=0.55±0.16 kcal/K mol are small for a protein of the size of BRCT. In agreement with the gel filtration chromatography results, the thermal unfolding of V1833M exhibits no T_m dependence upon C_t indicating that V1833M is in a monomeric native state [31] and thus the observed thermal unfolding is likely described similarly to the other two variants.

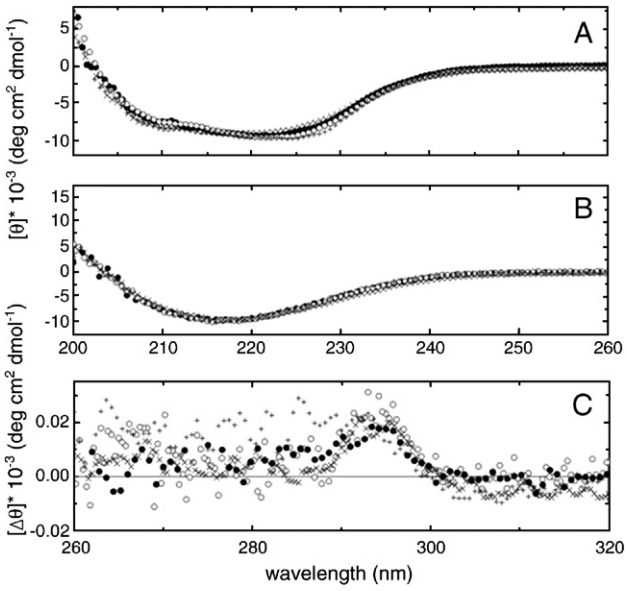

Fig. 4. (A) Normalized far-UV CD spectra wt-BRCT (○) [27], M1775R (●), R1699W (+) and V1833M (X) at 25 °C and (B) at 55 °C, approximately 10 degrees higher than the heat denaturation transition temperature T_m. (C) The difference $\Delta\theta$ vs. λ (native at 25 °C–denatured at 55 °C) near-UV CD spectra: The characteristic sharp, positive band centered at 295 nm can be associated to tryptophan residues.

3.2. CD spectroscopy

Previously published CD spectropolarimetric studies of the thermal unfolding of wt-BRCT at various values of pH and buffer conditions provided substantial evidence that the thermally denatured state retains most of the native's structural characteristics [27]. This observation is repeated for the variants studied here. As illustrated in Fig. 4A, the native CD far-UV spectra of all three variants perfectly overlap with the corresponding spectrum of wt-BRCT. Moreover, the far-UV CD spectra of all the denatured states, illustrated in Fig. 4B, also coincide considerably well. Comparing native and denatured spectra, it appears that the heat-induced alterations of the secondary structure elements of the native states are small (less than 6% loss in helical structure). More revealing though are the experimental results for the near-UV spectra depicting tertiary structure changes. As it is characteristically shown in Fig. 4C all the spectra $\Delta\theta$ (difference in ellipticity between the native and the denatured state) vs. λ, depicting changes in the molecule's tertiary structure, exhibit only a weak, yet distinct and fully reproducible anomaly at λ ~295 nm. This feature is thus providing additional evidence that the structural changes between the native and the denatured states are small for all the variants. In fact, considering the small enthalpic content of the DSC peaks, this feature can only be associated to thermally induced-changes in the environment of W1782 and W1712 residues located at the hydrophobic cleft between the two BRCT repeats and the inter-repeat linker [27]. Excess $\Delta\theta$ values observed in the case of R1699W variant in the region λ ~280 to 285 nm (Fig. 4C) are likely due to the additional tryptophan residue of this variant at position 1699.

3.3. ITC

The interactions of wt-BRCT with the BACH1 and the CtIP phosphopeptides have already been studied by ITC [13–16]. The wt-BRCT domain exhibits a higher affinity for BACH1 than CtIP. Here we have studied these interactions at pH 9.0, 5 mM sodium borate buffer, 200 mM NaCl for wt-BRCT as well as for the three variants and the thermally denatured molecules. Only wt-BRCT and V1833M were found to bind to both phosphopeptides. The interaction of the other two variants with either peptide showed no measurable heat and so did the interaction of the denatured molecules with either peptide. The ITC experimental data were analyzed via non-linear least-squares fits of the integrated heat vs. molar ratio to a single-site binding model. The fitting results are summarized in Table 3. The ITC plots for the interaction of wt-BRCT and V1833M variant with the two phosphopeptides are presented in Fig. 5. The results for wt-BRCT in pH 9.0 borate reveal a 5-fold higher affinity $k_a = 5.9 \pm 0.5 \times 10^6$ M^{-1} for binding to the BACH1 phosphopeptide than what was reported for the interaction at pH 7.5, 25 mM HEPES, 125 mM NaCl, where $k_a = 1.1 \times 10^6$ M^{-1} [14]. Moreover, the ITC results for the interaction of wt-BRCT domain with the CtIP phosphopeptide also lead to higher k_a values, $k_a = 7.6 \pm 1.3 \times 10^5$ M^{-1} than for the interaction in phosphate buffered saline, 300 mM NaCl, pH 7.4 where $k_a = 2.7 \times 10^5$ M^{-1} [16]. Analogously to pH 7.5, in solutions with pH 9.0, the wt-BRCT domain exhibits higher affinity for BACH1, than for CtIP. It has been argued that this may be related to the fact that residues in the neighborhood of pSer 0 and Phe +3 contribute differently to the binding affinity.

By contrast to M1775R and R1699W, the variant V1833M binds to both phosphopeptides. The data at pH 9.0, 5 mM sodium borate buffer, 200 mM NaCl, analyzed via a single-site binding model (Table 3) reveal that as in the case of wt-BRCT, V1833M exhibits a higher affinity for the BACH1 phosphopeptide $3.7 \pm 0.5 \times 10^6$ vs. $1.4 \pm 0.2 \times 10^6$ M^{-1}. Notably, in the case of V1833M the interaction with CtIP has a stronger binding constant than the corresponding one of wt-BRCT. The interaction of V1833M has also been probed at pH 7.0, 10 mM Na-phosphate buffer. ITC experiments with the BACH1 phosphopeptide reveal binding with $k_a = 1.2 \pm 0.6 \times 10^6$ M^{-1}, $N = 0.93$ and $\Delta H = 11.7 \pm 0.3$ kcal/mol. These results compare well with what has already been reported for the wild-type protein [14]. Finally, it is not surprising that no binding could be detected between molecules in the thermally denatured state and any of the two phosphopeptides.

Table 3
ITC results

Sample	N	(ΔH) (kcal/mol)	k_a ($\times 10^6$ M^{-1})
Binding to BACH1 phosphopeptide			
wt-BRCT	0.96	17.2±0.4	5.89±0.53
M1775R		No binding	
R1699W		No binding	
V1833M	0.94	16.0±0.3	3.72±0.50
Denatured molecules		No binding	
Binding to CtIP phosphopeptide			
wt-BRCT	0.94	10.9±0.3	0.76±0.13
M1775R		No binding	
R1699W		No binding	
V1833M	1.04	11.6±0.3	1.43±0.17
Denatured molecules		No binding	

Results obtained for fitting the ITC integrated heat data obtained at 20 °C in pH 9.0, 5 mM borate buffer, 200 mM NaCl, to a single binding site model.

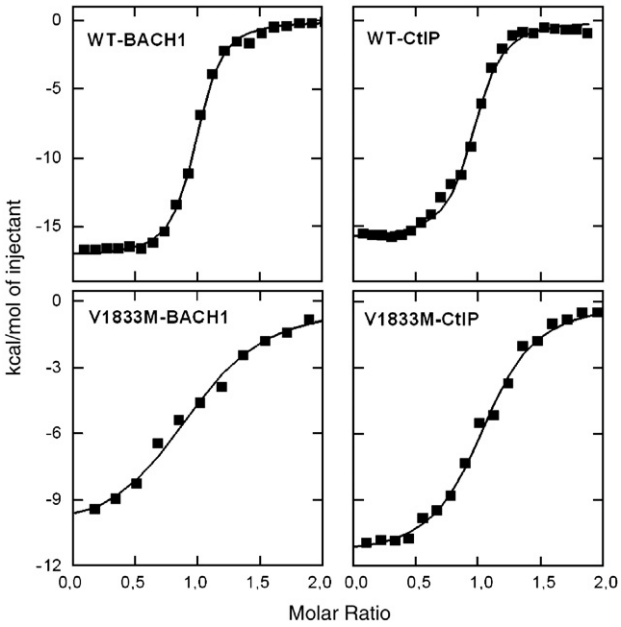

Fig. 5. Comparison of the interactions of wt-BRCT as well as of V1833M variant with the BACH1 and CtIP phosphopeptides. The isothermal plots are obtained at 20 °C in pH 9.0, 5 mM sodium borate buffer, 200 mM NaCl. The data presented are normalized, integrated heat data vs. molar ratio. The baseline of the exothermic heat pulses (raw data, not shown), as well as the peptide dilution heats have been subtracted. The solid lines are non-linear least-squares fits to a single-site binding model. Top left: wt-BRCT–BACH1 binding, top right: wt-BRCT–CtIP binding, bottom left: V1833M–BACH1 binding and bottom right: V1833M–CtIP binding. The fitting results are presented in Table 3.

Following the titration of wt-BRCT with the BACH1 phosphopeptide, additional DSC experiments were carried out for the thermal denaturation of the complex. At pH 9.0 borate buffer, protein concentration 0.0136 mM and peptide concentration 0.029 mM the DSC result was an irreversible endothermic peak at $T_m = 54.6$ °C with an enthalpy change $\Delta H = 84.9$ kcal/mol. The substantial increase, by ~6 °C, of T_m is likely an indication that the interaction of wt-BRCT with the phosphopeptide leads to a more thermodynamically stable state for the resulting complex. The DSC experiments of the complex also revealed the concentration-dependence of T_m, which in turn is an indication that upon denaturation the complex dissociates into the two constituents.

4. Discussion

For all the samples studied by DSC, the obtained per-residue values of the calorimetric parameters $(\Delta H)_{cal}$ and ΔC_p are small compared to globular proteins of same size [32,33]. This is indicative that limited structural changes take place during the observed thermal denaturation process. For wt-BRCT as well as

for the three variants the per-residue values of $(\Delta H)_{cal}$ varied between 220 and 400 cal/mol-residue and ΔC_p varied between 2.2 and 3.0 cal/K mol-residue. In fact, additional thermal unfolding may take place at higher T, not attained by the present experiments. Limited structural changes are also demonstrated for the thermal unfolding of all the molecules via the CD technique. It is thus straightforward to assume that the thermally denatured state observed by the present experiments is a partly unfolded aggregation-prone intermediate, which in contrast to the structureless intermediate evidenced by chemical denaturation experiments [26], retains most of the structural characteristics of the native. Apparently, the two intermediate states are unrelated because the thermal and chemical unfolding pathways lead to different denatured states.

Structure-based calculations of $(\Delta H)_{cal}$ and ΔC_p [34,35], on the heat denaturation of wt-BRCT have demonstrated that a good accord of the theoretical results with the experimentally measured values exists [27], when considering that partial unfolding and thermally-induced structural alterations occur mainly at the hydrophobic interface regions between the two BRCT repeats as well as at the interface between the BRCT repeats and the flexible inter-BRCT linker. It was specifically shown that the contribution to $(\Delta H)_{cal}$ from these interface regions amounts to $(\Delta H)_{cal}$=37.3 kcal/mol and to ΔC_p= 0.47 kcal/K mol at T=48 °C. It is evident that the calorimetric results presented here for the denaturation of M1775R, R1699W and V1833M variants are in relatively good agreement with the structure-based hypothesis The high-precision DSC results may thus provide substantial information on the likely mechanism of partial thermal unfolding. In addition to the calorimetric, the CD results presented here reveal that similarly to wt-BRCT, the observed thermal denaturation of the three variants destabilizes primarily the hydrophobic inter-BRCT repeat interface. While all the CD results though point towards a similar likely mechanism destabilizing the native fold, the DSC results reveal that the denaturation process itself is characterized by substantially different thermodynamic parameters, especially T_ms. Indeed, the various T_m values obtained for the BRCT variants display pronounced downwards drifts for M1775R and R1699W variants and a less substantial drift for V1833M.

Chemical denaturation studies of wt-BRCT and several variants including M1775R and V1833M revealed a two-step unfolding process [26]: First into an aggregation-prone almost structureless intermediate state and subsequently to the fully denatured state. The two mutants were found to have an equally major impact upon the stability of the wild-type with respect to the intermediate but no effect upon the stability of the intermediate with respect to the fully denatured state. No particular correlation could be established for specific sites of the BRCT domain and the destabilization induced by the respective sequence variants. In the present study, while the thermal unfolding of all three variants M1775R, R1699W and V1833M was shown to be characterized, similarly to wt-BRCT, by the presence of partly-folded, aggregation-prone denatured states, the three mutations reveal a different, site-dependent, impact upon the thermostability with respect to the partially unfolded thermal intermediates. Substantial decrease in the thermostability is recorded for M1775R and R1699W, while only moderate effects are exhibited in the case of V1833M. On the other hand evidence of enhanced stability is provided by the DSC results of the wt-BRCT/BACH1 phosphopeptide complex.

It was recently shown that irreversible thermal unfolding kinetic rates are linked with the thermostability of proteins in the case of fast irreversible processes [36]. For all the mutant proteins, studied here the analysis of the endothermic DSC peaks using an irreversible Lumry-Eyring model [31] yields activation enthalpy (E_α) values that are comparable ~47± 5 kcal/mol for M1775R and R1699W variants and considerably higher E_α ~74±5 kcal/mol for V1833M and E_α ~87± 4 kcal/mol for wt-BRCT. Once again, the effects of the mutations with respect to the wt-protein are found to be pronounced in the case of M1775R and R1699W and only mild in the case of variant V1833M.

Based on worldwide genetic screening data, missense mutations at the BRCT domain of human BRCA1, which have been argued to have a link with predisposition to hereditary breast/ovarian cancer, include M1775R and R1699W. The mutation M1775R has already been shown to induce subtle structural alteration only at the site of substitution with no impact upon the integrity of the overall BRCT domain structure [23]. Based on the calorimetric results presented here, it has the most severe effect upon the thermostability of the BRCT domain with respect to the thermally unfolded intermediate state. This, combined with the fact that the guanidinium group of Arg1775 obstructs Phe(+3) of the phosphopeptide pSer-X-X-Phe motif (of BACH1 and CtIP proteins) from accessing the binding pocket, renders this mutation capable of inactivating the BRCT domain and thus disease predisposing. Similarly to M1775R the mutation R1699W is only expected to have negligible effects upon the overall structure of the wild type. On the other hand, R1699W also has an important impact upon the BRCT domain's thermostability with respect to the thermal intermediate state as evidenced by the DSC results where a lowering of T_m by almost 8 degrees is evidenced. Since R1699W also affects the binding pocket of the phosphopeptide Phe at (+3) position, it is highly probable that it too leads to loss of function *in vivo*.

In the previously published chemical denaturation study it was shown that V1833M substantially destabilizes (by ~5.5 kcal/mol) the BRCT domain with respect to an almost completely unfolded intermediate state, as in fact does the mutation M1775R [26]. The calorimetric results of the present study however indicate that while M1775R has a serious impact, only moderate differences, relative to wt-BRCT, are encountered for the thermal unfolding of variant V1833M to the partially structured denatured state. The thermodynamic profiles for V1833M have considerably more similarities to wt-BRCT rather than to the corresponding ones for M1775R. Furthermore, the ITC experiments presented here demonstrate that V1833M interacts with both BACH1 and CtIP phosphopeptides.

Combination of proteolytic and computational techniques have demonstrated mutation-induced protein-destabilization

effects [37]. Crystallographic [13–16] and NMR [17] structural data have shown that biologically active BRCT conformations strongly depend upon the structural integrity as well as upon the alignment of the tandem BRCT repeats relative to each other. The thermal destabilization mechanism of the BRCT domain primarily involves the hydrophobic interface region between the two BRCT repeats and the flexible inter-repeat linker, which may directly lead to the loss of the molecule's function. It appears that mutations located at this hydrophobic cleft (M1775R, R1699W) have a much more pronounced impact upon the thermal unfolding parameters than V1833M where the missense mutation is distant from the inter-BRCT-repeat interface region. Notably, two additional mutations linked to the disease, A1708E and G1738R are located in this critical for the molecule's stability region, not directly interfering with the binding site. Ala1708 is a very well packed residue at the inter-BRCT-repeat interface. A glutamate at this position would cause serious charge and size incompatibility. Steric hindrance effects may induce exposure of the hydrophobic interface of the two BRCTs. It is thus highly probable that A1708E severely destabilizes the BRCT domain structure leading to loss of function. Indeed, this may be the reason why several attempts to purify A1708E variant in a soluble form have failed, since unfolded states exhibit a very high propensity for aggregation. Analogous may also be the effects of G1738R a mutation detected in patients of Greek descent [38]. Interestingly, Gly1738 is conserved among BRCA1s and is structurally conserved in 53BP1 proteins that also contain a tandem of BRCT repeats. It is located at a loop of the inter-BRCT linker in the vicinity of the binding site. Replacement by an Arginine is anticipated to induce alterations leading to the likely exposure of the hydrophobic inter-BRCT interface affecting the overall shape of the binding surface.

The experimental results presented here, provide a measure of the severity by which some thermodynamic properties of the BRCA1 BRCT domain are affected by selected missense mutations. They also provide a strong indication that in addition to structural alterations at the binding pockets, the mutation-induced destabilization of the hydrophobic inter-BRCT-repeat region is crucial for the structural integrity of the domain and consequently for its ability for peptide recognition. The thermal unfolding profiles of variant V1833M demonstrate that the mutation does affect the variant's thermostability with respect to the wild-type albeit not as strongly as the cancer-linked mutations M1775R and R1699W. On the other hand the present thermodynamic results reveal that the binding of V1833M with the BACH1 and CtIP phosphopeptides is analogous to wild-type. The association of this variant with hereditary breast/ovarian cancer in terms of thermodynamic stability arguments may thus be premature.

Acknowledgements

G.N., S.P., and A.T. acknowledge support from the Graduate Fellowship Program of NCSR "Demokritos". We would like to thank Prof. A. Monteiro for kindly providing the BRCT plasmids. The use of the CD facilities at the Centre for Crystallographic Studies of Macromolecules of NCSR "Demokritos" is acknowledged. This work was supported by funding from the General Secretariat of Research and Technology of Greece, Excellence in Research II, funded by 75% from the European Union.

References

[1] Y. Miki, J. Swensen, D. Shattuck-Eidens, P.A. Futreal, K. Harshman, S. Tavtigian, Q. Liu, C. Cochran, L.M. Bennett, W. Ding, et al., A strong candidate for the breast and ovarian cancer susceptibility gene BRCA1, Science 266 (1994) 66–71.
[2] P.A. Futreal, Q. Liu, D. Shattuck-Eidens, C. Cochran, K. Harshman, S. Tavtigian, L.M. Bennett, A. Haugen-Strano, J. Swensen, Y. Miki, et al., BRCA1 mutations in primary breast and ovarian carcinomas, Science 266 (1994) 120–122.
[3] N. Mirkovic, M.A. Marti-Renom, B.L. Weber, A. Sali, A.N. Monteiro, Structure-based assessment of missense mutations in human BRCA1: implications for breast and ovarian cancer predisposition, Cancer Res. 64 (2004) 3790–3797.
[4] F. Hayes, C. Cayanan, D. Barilla, A.N. Monteiro, Functional assay for BRCA1: mutagenesis of the COOH-terminal region reveals critical residues for transcription activation, Cancer Res. 60 (2000) 2411–2418.
[5] A.N. Monteiro, A. August, H. Hanafusa, Common BRCA1 variants and transcriptional activation, Am. J. Hum. Genet. 61 (1997) 761–762.
[6] J.S. Humphrey, A. Salim, M.R. Erdos, F.S. Collins, L.C. Brody, R.D. Klausner, Human BRCA1 inhibits growth in yeast: potential use in diagnostic testing, Proc. Natl. Acad. Sci. U. S. A. 94 (1997) 5820–5825.
[7] R.S. Williams, R. Green, J.N. Glover, Crystal structure of the BRCT repeat region from the breast cancer-associated protein BRCA1, Nat. Struct. Biol. 8 (2001) 838–842.
[8] D.J. Derbyshire, B.P. Basu, L.C. Serpell, W.S. Joo, T. Date, K. Iwabuchi, A.J. Doherty, Crystal structure of human 53BP1 BRCT domains bound to p53 tumour suppressor, EMBO J. 21 (2002) 3863–3872.
[9] M. Rodriguez, X. Yu, J. Chen, Z. Songyang, Phosphopeptide binding specificities of BRCA1 COOH-terminal (BRCT) domains, J. Biol. Chem. 278 (2003) 52914–52918.
[10] X. Yu, C.C. Chini, M. He, G. Mer, J. Chen, The BRCT domain is a phospho-protein binding domain, Science 302 (2003) 639–642.
[11] X. Yu, R. Baer, Nuclear localization and cell cycle-specific expression of CtIP, a protein that associates with the BRCA1 tumor suppressor, J. Biol. Chem. 275 (2000) 18541–18549.
[12] X. Yu, J. Chen, DNA damage-induced cell cycle checkpoint control requires CtIP, a phosphorylation-dependent binding partner of BRCA1 C-terminal domains, Mol. Cell Biol. 24 (2004) 9478–9486.
[13] J.A. Clapperton, I.A. Manke, D.M. Lowery, T. Ho, L.F. Haire, M.B. Yaffe, S.J. Smerdon, Structure and mechanism of BRCA1 BRCT domain recognition of phosphorylated BACH1 with implications for cancer, Nat. Struct. Mol. Biol. 11 (2004) 512–518.
[14] E.N. Shiozaki, L. Gu, N. Yan, Y. Shi, Structure of the BRCT repeats of BRCA1 bound to a BACH1 phosphopeptide: implications for signaling, Mol. Cell 14 (2004) 405–412.
[15] R.S. Williams, M.S. Lee, D.D. Hau, J.N. Glover, Structural basis of phosphopeptide recognition by the BRCT domain of BRCA1, Nat. Struct. Mol. Biol. 11 (2004) 519–525.
[16] A.K. Varma, R.S. Brown, G. Birrane, J.A. Ladias, Structural basis for cell cycle checkpoint control by the BRCA1-CtIP complex, Biochemistry 44 (2005) 10941–10946.
[17] M.V. Botuyan, Y. Nomine, X. Yu, N. Juranic, S. Macura, J. Chen, G. Mer, Structural basis of BACH1 phosphopeptide recognition by BRCA1 tandem BRCT domains, Structure (Camb.) 12 (2004) 1137–1146.
[18] A.N. Monteiro, A. August, H. Hanafusa, Evidence for a transcriptional activation function of BRCA1 C-terminal region, Proc. Natl. Acad. Sci. U. S. A. 93 (1996) 13595–13599.
[19] M.S. Chapman, I.M. Verma, Transcriptional activation by BRCA1, Nature 382 (1996) 678–679.

[20] S.B. Cantor, D.W. Bell, S. Ganesan, E.M. Kass, R. Drapkin, S. Grossman, D.C. Wahrer, D.C. Sgroi, W.S. Lane, D.A. Haber, D.M. Livingston, BACH1, a novel helicase-like protein, interacts directly with BRCA1 and contributes to its DNA repair function, Cell 105 (2001) 149–160.
[21] S. Li, P.L. Chen, T. Subramanian, G. Chinnadurai, G. Tomlinson, C.K. Osborne, Z.D. Sharp, W.H. Lee, Binding of CtIP to the BRCT repeats of BRCA1 involved in the transcription regulation of p21 is disrupted upon DNA damage, J. Biol. Chem. 274 (1999) 11334–11338.
[22] X. Yu, L.C. Wu, A.M. Bowcock, A. Aronheim, R. Baer, The C-terminal (BRCT) domains of BRCA1 interact in vivo with CtIP, a protein implicated in the CtBP pathway of transcriptional repression, J. Biol. Chem. 273 (1998) 25388–25392.
[23] R.S. Williams, J.N. Glover, Structural consequences of a cancer-causing BRCA1-BRCT missense mutation, J. Biol. Chem. 278 (2003) 2630–2635.
[24] A. Ladopoulou, C. Kroupis, I. Konstantopoulou, L. Ioannidou-Mouzaka, A.C. Schofield, A. Pantazidis, S. Armaou, I. Tsiagas, E. Lianidou, E. Efstathiou, C. Tsionou, C. Panopoulos, M. Mihalatos, G. Nasioulas, D. Skarlos, N.E. Haites, G. Fountzilas, N. Pandis, D. Yannoukakos, Germ line BRCA1 and BRCA2 mutations in Greek breast/ovarian cancer families: 5382insC is the most frequent mutation observed, Cancer Lett. 185 (2002) 61–70.
[25] T. Huyton, P.A. Bates, X. Zhang, M.J. Sternberg, P.S. Freemont, The BRCA1 C-terminal domain: structure and function, Mutat. Res. 460 (2000) 319–332.
[26] C.M. Ekblad, H.R. Wilkinson, J.W. Schymkowitz, F. Rousseau, S.M. Freund, L.S. Itzhaki, Characterisation of the BRCT domains of the breast cancer susceptibility gene product BRCA1, J. Mol. Biol. 320 (2002) 431–442.
[27] S. Pyrpassopoulos, A. Ladopoulou, M. Vlassi, Y. Papanikolau, C.E. Vorgias, D. Yannoukakos, G. Nounesis, Thermal denaturation of the BRCT tandem repeat region of human tumour suppressor gene product BRCA1, Biophys. Chem. 114 (2005) 1–12.
[28] U.K. Laemmli, Cleavage of structural proteins during the assembly of the head of bacteriophage T4, Nature 227 (1970) 680–685.
[29] V.V. Plotnikov, J.M. Brandts, L.N. Lin, J.F. Brandts, A new ultrasensitive scanning calorimeter, Anal. Biochem. 250 (1997) 237–244.
[30] K. Takahashi, J.M. Sturtevant, Thermal denaturation of streptomyces subtilisin inhibitor, subtilisin BPN′, and the inhibitor–subtilisin complex, Biochemistry 20 (1981) 6185–6190.
[31] J.M. Sanchez-Ruiz, Theoretical-analysis of Lumry–Eyring models in differential scanning calorimetry, Biophys. J. 61 (1992) 921–935.
[32] M.W. Lassalle, H.J. Hinz, H. Wenzel, M. Vlassi, M. Kokkinidis, G. Cesareni, Dimer-to-tetramer transformation: loop excision dramatically alters structure and stability of the ROP four alpha-helix bundle protein, J. Mol. Biol. 279 (1998) 987–1000.
[33] C.G. Benitez-Cardoza, A. Rojo-Dominguez, A. Hernandez-Arana, Temperature-induced denaturation and renaturation of triosephosphate isomerase from *Saccharomyces cerevisiae*: evidence of dimerization coupled to refolding of the thermally unfolded protein, Biochemistry 40 (2001) 9049–9058.
[34] J. Gomez, V.J. Hilser, D. Xie, E. Freire, The heat capacity of proteins, Proteins 22 (1995) 404–412.
[35] V.J. Hilser, J. Gomez, E. Freire, The enthalpy change in protein folding and binding: refinement of parameters for structure-based calculations, Proteins 26 (1996) 123–133.
[36] C. Duy, J. Fitter, Thermostability of irreversible unfolding alpha-amylases analyzed by unfolding kinetics, J. Biol. Chem. 280 (2005) 37360–37365.
[37] R.S. Williams, D.I. Chasman, D.D. Hau, B. Hui, A.Y. Lau, J.N. Glover, Detection of protein folding defects caused by BRCA1-BRCT truncation and missense mutations, J. Biol. Chem. 278 (2003) 53007–53016.
[38] G. Chenevix-Trench, S. Healey, S. Lakhani, P. Waring, M. Cummings, R. Brinkworth, A.M. Deffenbaugh, L.A. Burbidge, D. Pruss, T. Judkins, T. Scholl, A. Bekessy, A. Marsh, P. Lovelock, M. Wong, A. Tesoriero, H. Renard, M. Southey, J.L. Hopper, K. Yannoukakos, M. Brown, D. Easton, S.V. Tavtigian, D. Goldgar, A.B. Spurdle, Genetic and histopathologic evaluation of BRCA1 and BRCA2 DNA sequence variants of unknown clinical significance, Cancer Res. 66 (2006) 2019–2027.